

# Single-Walled Carbon Nanotubes in the Intact Organism: Near-IR Imaging and Biocompatibility Studies in *Drosophila*

Tonya K. Leeuw,<sup>†</sup> R. Michelle Reith,<sup>‡</sup> Rebecca A. Simonette,<sup>‡</sup>  
Mallory E. Harden,<sup>‡,§</sup> Paul Cherukuri,<sup>†</sup> Dmitri A. Tsyboulski,<sup>†</sup>  
Kathleen M. Beckingham,<sup>\*,‡</sup> and R. Bruce Weisman<sup>\*,†</sup>

Department of Chemistry, Department of Biochemistry and Cell Biology,  
Center for Biological and Environmental Nanotechnology, R. E. Smalley Institute for  
Nanoscale Science and Technology, and Institute for Biosciences and Bioengineering,  
Rice University, 6100 Main Street, Houston, Texas 77005

Received May 3, 2007; Revised Manuscript Received July 5, 2007

## ABSTRACT

The ability of near-infrared fluorescence imaging to detect single-walled carbon nanotubes (SWNTs) in organisms and biological tissues has been explored using *Drosophila melanogaster* (fruit flies). *Drosophila* larvae were raised on food containing ~10 ppm of disaggregated SWNTs. Their viability and growth were not reduced by nanotube ingestion. Near-IR nanotube fluorescence was imaged from intact living larvae, and individual nanotubes in dissected tissue specimens were imaged, structurally identified, and counted to estimate a biodistribution.

Single-walled carbon nanotubes (SWNTs) are attracting increasing attention in biomedical research because their unique physical and chemical properties offer the promise of novel diagnostic and therapeutic methods.<sup>1–5</sup> In developing such applications, the challenges of in vivo detection and biocompatibility must be addressed. We report here the results of a study in which larvae of *Drosophila melanogaster* (fruit flies) were fed food containing water-solubilized, pristine SWNTs. We utilized the intrinsic near-infrared (NIR) fluorescence of SWNTs to capture the first optical images of nanotubes inside a living organism. Dissected tissues were examined by NIR fluorescence microscopy, allowing individual incorporated SWNTs to be observed, structurally identified, and counted. From such observations, we compiled a biodistribution showing variations of nanotube concentrations among tissues. In addition, the viability and growth of the exposed flies were monitored and compared to those of control groups.

SWNTs are a family of tubular nanostructures formed from covalently bonded carbon atoms. They exist as a variety of structural species that differ in diameter and chiral angle, each uniquely identified by a pair of integers,  $(n,m)$ .<sup>6</sup>

Approximately two-thirds of SWNT species are electronic semiconductors. When they are not aggregated or chemically altered, these semiconducting SWNTs show band gap fluorescent emission in the NIR spectral region at wavelengths characteristic of their specific  $(n,m)$  structure.<sup>7,8</sup> The SWNTs used here have typical diameters of 1 nm and lengths of several hundred nanometers; they emit light between 900 and 1600 nm. Because natural biomolecules are relatively transparent and nonemissive in this range, the sharp spectra of SWNTs can be detected even in complex biological environments. It was previously demonstrated that SWNT intrinsic fluorescence can be observed and imaged after uptake into cultured macrophage cells and that SWNTs produced no adverse effects on viability of these cultures.<sup>9</sup> A recent rabbit study used NIR fluorescence to monitor SWNT pharmacokinetics following intravenous administration.<sup>10</sup> Nanotube fluorescence is also being used in novel biomedical sensor research.<sup>11,12</sup> As a step toward developing biomedical applications based on nanotube fluorescence, we have explored the effects and fate of SWNTs orally administered to *Drosophila melanogaster*, the preeminent model organism of biology.

Given concerns about the toxicity of SWNTs in whole organisms, we first investigated the effects on overall viability and growth of feeding SWNTs to larvae throughout their entire growth phase. After hatching from the egg case, *Drosophila* larvae undergo an intense 4–5 day feeding period in which they increase in weight 200-fold. During the

\* Corresponding authors. E-mail: weisman@rice.edu (R.B.W.); kate@bioc.rice.edu (K.M.B.). Telephone: 713-348-3709 (R.B.W.); 713-348-4016 (K.M.B.). Fax: 713-348-5155 (R.B.W.); 713-348-5154 (K.M.B.).

<sup>†</sup> Department of Chemistry.

<sup>‡</sup> Department of Biochemistry and Cell Biology.

<sup>§</sup> Present address: Trinity University, One Trinity Place, San Antonio, Texas 78212.

subsequent immobile pupal phase, there is no feeding, so the weight of adults newly emerged from their pupal cases directly reflects their larval growth. To feed larvae the highest possible doses of SWNTs, dry Baker's yeast (the normal food) was mixed with concentrated suspensions of SWNTs in buffered bovine serum albumin (BSA) solutions. These suspensions were prepared by ultrasonic dispersion of raw HiPco SWNTs into a phosphate-buffered saline solution of BSA, followed by centrifugation and decantation (see Supporting Information). The resulting pastes (which differed somewhat in nanotube content) were used as the sole food source for various batches of larvae. Survival to the pupal and adult stages for larvae fed exclusively on such a SWNT yeast paste containing 9 ppm SWNTs was quantitated and compared to survival of larvae fed a control paste prepared from nanotube-free BSA buffer. As shown in Figure 1a, we found that SWNT feeding did not affect survival to either stage. In fact, survival to pupal stage and adulthood was somewhat higher for the SWNT-fed group ( $83.5 \pm 3.8\%$  versus  $78.0 \pm 3.9\%$  to the pupal stage, and  $79.5 \pm 3.4\%$  versus  $69.4 \pm 3.9\%$  to the adult stage), with the survival difference to adulthood showing statistical significance ( $p < 0.006$ ). To determine whether SWNTs affect overall growth, comparable experiments were performed in which newly emerged adults were sorted by sex and their masses measured. Figure 1b compares masses for groups of adults grown on two different concentrations of SWNTs. As is normal for *Drosophila*, females weigh more than males in both groups, but no significant differences were detected when comparing control and nanotube-fed individuals.

We next investigated in vivo detection of SWNTs in nanotube-fed larvae using a custom-built NIR fluorescence microscope. This instrument used diode lasers at 658 and 785 nm for sample excitation and an InGaAs array detector for NIR imaging (see Supporting Information). NIR fluorescence from SWNTs was readily imaged in the digestive tracts of intact, living larvae fed on SWNT yeast paste (Figure 2a). Videos constructed from NIR fluorescence image sequences clearly show peristaltic movements in the digestive system (see Supporting Information). Figure 2b displays one frame from such a sequence, with NIR emission intensity coded by false color. The glowing loop structure is the gut of the larva illuminated by ingested nanotubes passing through the digestive system. As is estimated below, only a tiny fraction of these SWNTs become incorporated into tissues. We believe this to be the first demonstration of nanotube imaging from within a living organism, and it clearly suggests the potential of SWNT fluorescence methods for diagnostic applications.

To determine whether any of the ingested SWNTs actually traverse the gut wall and enter the interior of the larvae, individual tissues were removed, fixed, and scanned for NIR fluorescence. In *Drosophila*, all internal organs are bathed in the hemolymph, a blood equivalent. Hemolymph circulates through an open vessel (the dorsal vessel) that pumps fluid from the posterior body cavity by using a series of valves to prevent backflow. The vessel passes between the two brain hemispheres and discharges fluid into the anterior of the larva.

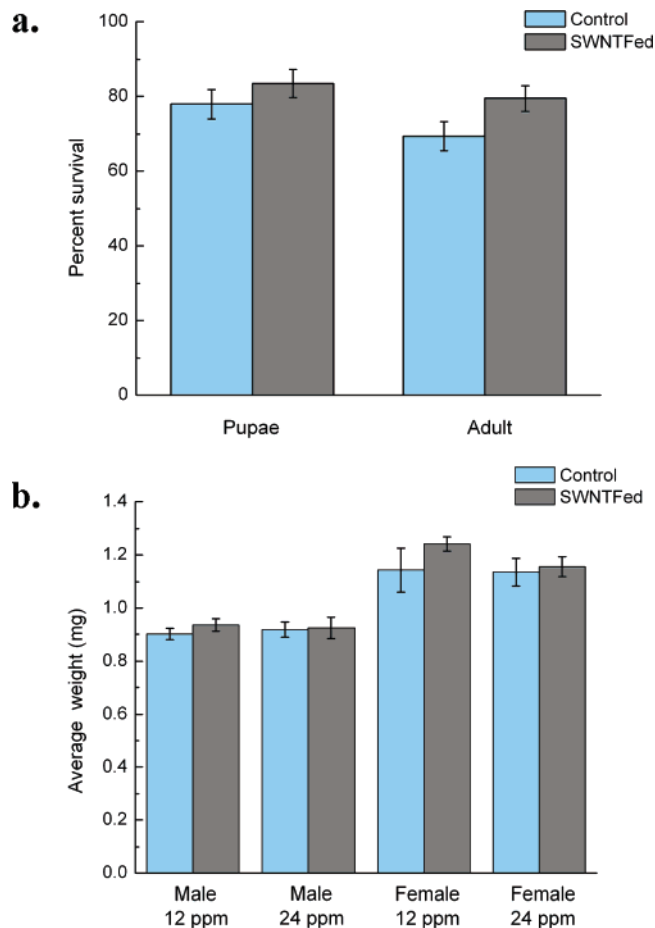


**Figure 1.** Viability and growth of SWNT-fed *Drosophila*. (a) Comparison of survival rates to the pupal and adult stages for *Drosophila* fed throughout the larval period exclusively on yeast paste containing SWNTs (9 ppm) or on control paste. Each group contained 10 batches of 20 larvae. The slightly greater survival rate to adult stage for the SWNT-fed larvae is significant ( $p < 0.006$ ) in a paired Student's t-test. (b) Average weights of newly eclosed flies fed throughout the larval period exclusively on control yeast paste or yeast paste with one of two concentrations of SWNT (12 or 24 ppm). Flies were weighed in batches of 10. Total numbers weighed: 130 for control and 12 ppm SWNT-fed males; 60 for control and 12 ppm SWNT-fed females; 90 for control and 24 ppm SWNT-fed males; 60 for control and 24 ppm SWNT-fed females. Differences are significant between males and females but not between control and SWNT-fed groups, including the females fed 12 ppm SWNTs.

High concentrations of nanotube fluorescence were observed in a tubelike structure associated with the brain lobes. We verified that this was the dorsal vessel by use of a fly strain that expresses green fluorescent protein (GFP) uniquely in this structure.<sup>13</sup> As shown in Figure 2c–e, the GFP fluorescence allowed us to confirm that nanotubes accumulate in the lumen of the dorsal vessel. We propose that, after traversing the gut wall, nanotubes in the hemolymph accumulate in the dorsal vessel as a result of its pumping action.

Apart from the strong SWNT NIR fluorescence seen from the gut and dorsal vessel, much lower levels of nanotube fluorescence were detected in all other tissues examined. This emission generally appeared as discrete spots in NIR fluorescence microscopy. We established that these spots

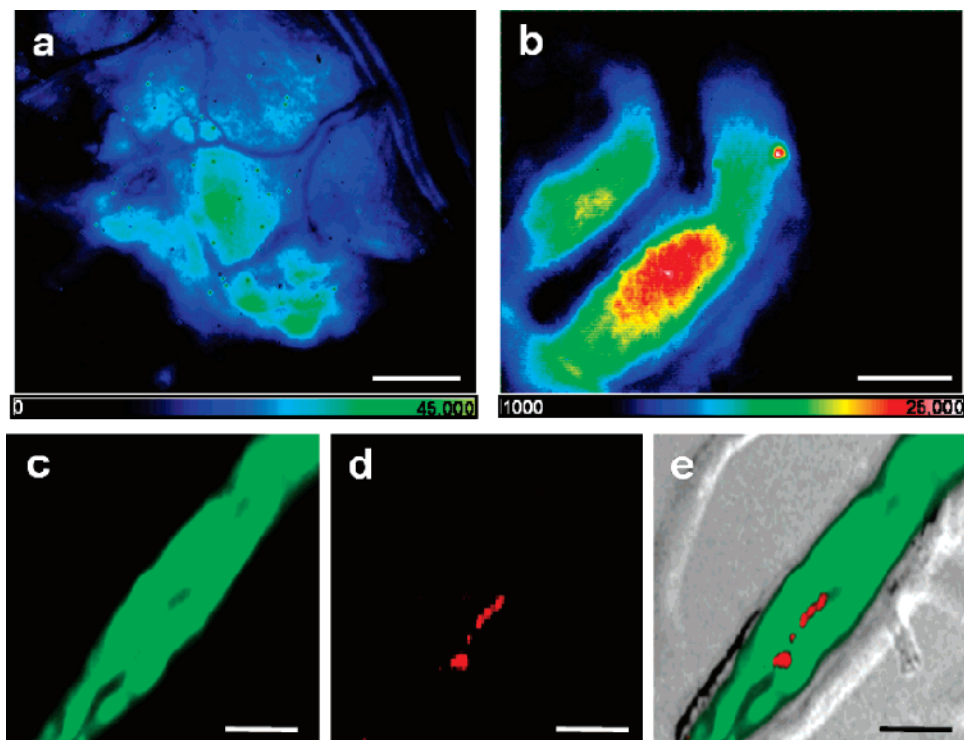


**Figure 2.** SWNTs in the gut and blood system. (a,b) NIR emission (color-coded for intensity) from SWNTs in the gut of a living larva viewed through the larval cuticle. In (a), the black branching structures are part of the trachea system that brings air in from openings in the cuticle surface (upper right). The larva was fed yeast paste containing 9 ppm SWNTs. (b) Boluses of food containing SWNTs in a loop of the gut of a living larva. This 0.5 s exposure was from a sequence that clearly showed peristaltic activity. Scale bars are 50  $\mu\text{m}$  (a) and 100  $\mu\text{m}$  (b). Note that the experimental conditions and intensity scales differ for (a) and (b). (c–e) SWNT NIR emission showing accumulation in the dorsal vessel. Green fluorescence from GFP expressed exclusively in the dorsal vessel is shown in panel (c), and NIR fluorescence from nanotubes is shown in panel (d) (false colored in red). (e) Overlay of these two images on the corresponding bright field image, demonstrating that the SWNTs lie within the lumen of the vessel. Scale bars are 25  $\mu\text{m}$ . For (b–e), larvae were fed yeast paste containing 16 ppm SWNTs.

corresponded to single nanotubes through two tests. First, the intensity of each spot's emission showed a strong dependence on the polarization orientation of the excitation beam. This is expected for single nanotubes because of their highly anisotropic optical transitions.<sup>14,15</sup> Second, the emission spectra of individual spots revealed single clear peaks characteristic of specific semiconducting SWNT species. Figure 3 shows images of individual nanotubes embedded in the larval ventral nerve cord (a component of the central nervous system). Emission spectra of the two spots labeled 1 and 2 in Figure 3b are plotted in Figure 3c. These are clearly the spectra of single SWNTs, with peak positions falling within the inhomogeneous widths of assigned bands in the bulk SWNT sample. We could thereby identify nanotube 1 as a (8,3) species and nanotube 2 as a (7,5). The average mass of these individual nanoparticles is approximately  $6 \times 10^{-19}$  g.

To determine the distribution of SWNTs among different tissues, we examined several larval organs by NIR fluorescence microscopy and counted emissive SWNTs in each specimen. At least four samples of each organ type were scored from larvae fed on yeast paste containing 16 ppm SWNT (prepared from a 25 mg/L aqueous suspension of SWNTs in BSA). The average concentrations, expressed as nanotubes per  $\text{mm}^3$  of tissue, were:  $900 \pm 550$  in the brain lobes and ventral nerve cord,  $300 \pm 180$  in the imaginal

discs,  $3100 \pm 450$  in the salivary gland,  $1300 \pm 190$  in the Malpighian tubes,  $75 \pm 40$  in the trachea, and  $40 \pm 30$  in the fat body. These values correspond to SWNT mass fractions in the  $10^{-12}$  range but do not include metallic SWNTs, which although present in our sample cannot be detected by NIR fluorescence. To account for these “invisible” nanotubes, we have applied an estimated correction factor of 1.5. The resulting biodistribution is shown as a chart in Figure 4. Using these results, we estimate that the fraction of ingested nanotubes that became incorporated into larval organs is on the order of  $10^{-8}$ . Therefore, nearly all of the nanotubes giving strong NIR emission from the gut (Figure 2b) became excreted rather than absorbed.

The relatively high level of SWNTs in the salivary glands probably reflects the close connection of these glands with the digestive system. It seems possible that SWNTs entered the salivary glands by backflow from the gut. Similarly, the few SWNTs in the trachea (a branching system of air-filled tubes with direct terminal openings to the exterior) may have entered not from the circulating hemolymph but rather through SWNT attachment to the larval cuticle as the animals burrowed through their food. For two of the remaining tissues, CNS and imaginal discs, the presence of SWNTs most probably represents secondary uptake after entry of SWNTs into the hemolymph.<sup>16</sup> The Malpighian tubules are analogous to the mammalian kidney and are known to

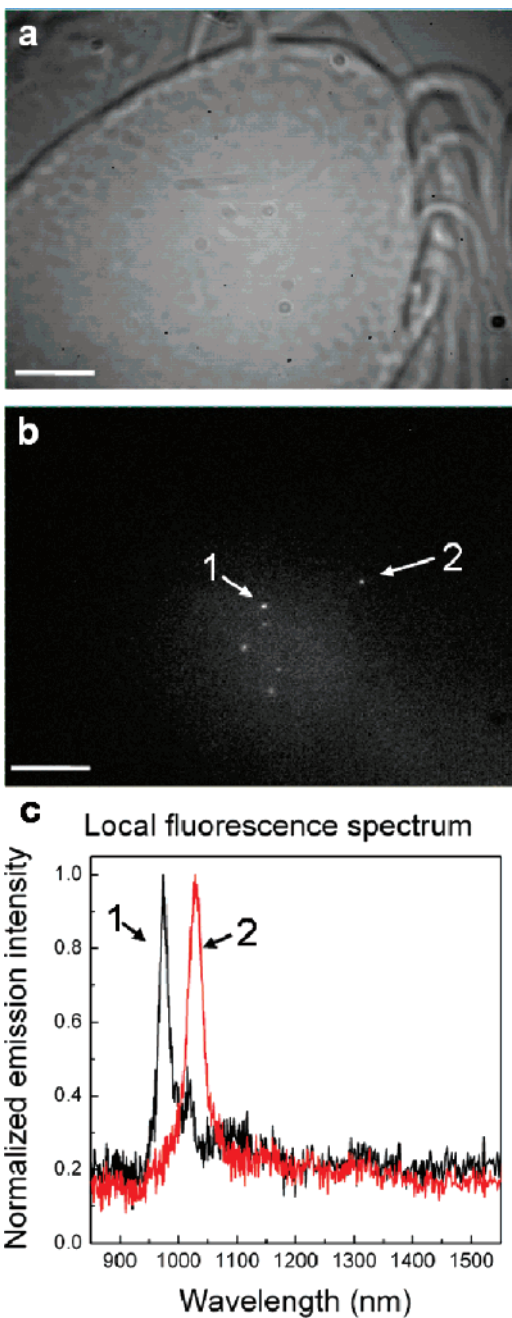


**Figure 3.** Optical detection of individual nanotubes in the *Drosophila* central nervous system. (a) Bright-field image of a larval ventral nerve cord and attached nerves. (b) Corresponding NIR emission image from this organ. Scale bars are 25  $\mu\text{m}$ . (c) Emission spectra of the features labeled 1 and 2 in (b), showing the clear spectral signatures of individual SWNTs. The peak positions indicate that these nanotubes are (8,3) and (7,5) structures, respectively. The larva was fed food containing 16 ppm SWNTs.

express organic solute transporters with the potential to excrete a broad range of xenobiotic compounds that accumulate in the hemolymph.<sup>16</sup> However, these tubules are also directly connected to the digestive tract and food-derived parasites can be sequestered in their upper reaches.<sup>16,17</sup> Thus, the SWNTs found in the Malpighian tubules may reflect either direct uptake from the hemolymph for excretion or backflow from the digestive tract.

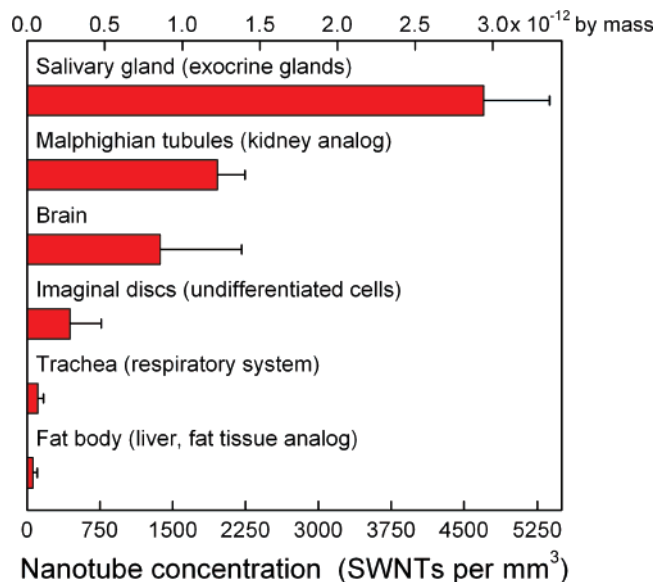


**Figure 4.** Organ distribution of SWNTs in *Drosophila* larvae fed with food containing 16 ppm SWNTs. Bars show SWNT concentrations deduced by counting individual fluorescent nanotubes (see Figure 3) in selected organs of *Drosophila* larvae. Observed values have been multiplied by a factor of 1.5 to correct for the presence of nonemissive metallic nanotube species. Error bars show SEMs. Mammalian equivalents to the larval organs are given in parentheses.

Our study addresses two issues relevant to envisioned applications of SWNTs. First, it demonstrates that NIR fluorescence is a highly effective probe for disaggregated SWNTs in biological tissues and organisms. It can detect, image, and structurally identify individual nanotubes in tissue specimens and can nondestructively image accumulations of nanotubes inside living organisms. Second, our study provides new results on the effect of SWNTs on intact organisms, relevant to possible medical uses and also to environmental contamination concerns.<sup>18,19</sup> We found no short-term toxicity or impaired growth or viability of *Drosophila* larvae that had been fed dispersed SWNTs at the highest concentrations attainable by our methods. In addition, there was no obvious impairment of fertility in matured SWNT-fed individuals. Although we cannot exclude subtle effects on some aspects of the *Drosophila* life cycle, our findings suggest that SWNTs ingested by these insects will have negligible physiological impact. Further, we estimate that only a very small fraction,  $\sim 10^{-8}$ , of the ingested nanotubes became incorporated into organs of the larvae. If these findings are valid for other insect species, then uptake by insect ingestion may prove to be an ineffective route for nanotube entry into the food chain from the environment. In summary, the sensitive *in vivo* detection and apparent biocompatibility of single-walled carbon nanotubes shown here support their promise for the development of novel biomedical applications.

**Acknowledgment.** This research has been supported by the NSF (CHE-0314270), the Alliance for NanoHealth (NASA NNJ05HE75A), the NSF Center for Biological and Environmental Nanotechnology (EEC-0118007), and the

Welch Foundation (grants C-0807 to R.B.W. and C-1119 to K.M.B.). We are also grateful to S. W. Casscells, III, and J. L. Conyers (University of Texas Health Science Center, Houston) for instrumentation support. D.A.T. thanks the Welch Foundation for postdoctoral fellowship support (L-C-0004).

**Supporting Information Available:** Details of materials and methods, and a video file (AVI) showing SWNT fluorescence emission imaged in a living larva. This material is available free of charge via the Internet at <http://pubs.acs.org>.

## References

- (1) Bianco, A.; Kostarelos, K.; Prato, M. *Curr. Opin. Chem. Biol.* **2005**, *9*, 674–679.
- (2) Kam, N. W. S.; O'Connell, M. J.; Wisdom, J. A.; Dai, H. *Proc. Natl. Acad. Sci. U.S.A.* **2005**, *102*, 11600–11605.
- (3) Kam, N. W. S.; Dai, H. *J. Am. Chem. Soc.* **2005**, *127*, 6021–6026.
- (4) Lin, Y.; Taylor, S.; Li, H.; Shiral Fernando, K. A.; Qu, L.; Wang, W.; Gu, L.; Zhou, B.; Sun, Y.-P. *J. Mater. Chem.* **2004**, *14*, 527–541.
- (5) Lacerda, L.; Bianco, A.; Prato, M.; Kostarelos, K. *Adv. Drug Delivery Rev.* **2006**, *58*, 1460–1470.
- (6) Saito, R.; Dresselhaus, G.; Dresselhaus, M. S. *Physical Properties of Carbon Nanotubes*; Imperial College Press: London, 1998.
- (7) O'Connell, M.; Bachilo, S. M.; Huffman, C. B.; Moore, V.; Strano, M. S.; Haroz, E.; Rialon, K.; Boul, P. J.; Noon, W. H.; Kittrell, C.; Ma, J.; Hauge, R. H.; Weisman, R. B.; Smalley, R. E. *Science* **2002**, *297*, 593–596.
- (8) Bachilo, S. M.; Strano, M. S.; Kittrell, C.; Hauge, R. H.; Smalley, R. E.; Weisman, R. B. *Science* **2002**, *298*, 2361–2366.
- (9) Cherukuri, P.; Bachilo, S. M.; Litovsky, S. H.; Weisman, R. B. *J. Am. Chem. Soc.* **2004**, *126*, 15638–15639.
- (10) Cherukuri, P.; Gannon, C. J.; Leeuw, T. K.; Schmidt, H. K.; Smalley, R. E.; Curley, S. A.; Weisman, R. B. *Proc. Natl. Acad. Sci. U.S.A.* **2006**, *103*, 18882–18886.
- (11) Barone, P. W.; Baik, S.; Heller, D. A.; Strano, M. S. *Nat. Mater.* **2005**, *4*, 86–92.
- (12) Heller, D. A.; Baik, S.; Eurell, T. E.; Strano, M. S. *Adv. Mater.* **2005**, *17*, 2793–2799.
- (13) Kimbrell, D. A.; Hice, C.; Bolduc, C.; Kleinhesselink, K.; Beckingham, K. *Genesis* **2002**, *34*, 23–28.
- (14) Lefebvre, J.; Fraser, J. M.; Finnie, P.; Homma, Y. *Phys. Rev. B* **2004**, *69*, 075403-1–075403-5.
- (15) Tsyboulski, D. A.; Bachilo, S. M.; Weisman, R. B. *Nano Lett.* **2005**, *5*, 975–979.
- (16) Dow, J. A. T.; Davies, S. A. *J. Insect Physiol.* **2006**, *52*, 365–378.
- (17) Dow, J. A. T., personal communication.
- (18) Warheit, D. B. *Carbon* **2006**, *44*, 1064–1069.
- (19) Lam, C. W.; James, J. T.; McCluskey, R.; Arepalli, S.; Hunter, R. L. *Crit. Rev. Toxicol.* **2006**, *36*, 189–217.

NL0710452